

## Influence of the bound nucleotide on the molecular dynamics of actin

György HEGYI<sup>1</sup>, László SZILÁGYI<sup>1</sup> and József BELÁGYI<sup>2</sup>

<sup>1</sup> Department of Biochemistry, Eötvös Loránd University

<sup>2</sup> Central Laboratory, Medical University of Pécs

(Received February 2/March 29, 1988) – EJB 88 0140

Rotational dynamics of actin spin-labelled with maleimide probes at the reactive thiol Cys-374 were studied. Replacement of the bound nucleotide by Br<sup>8</sup>ATP in G-actin and Br<sup>8</sup>ADP in F-actin causes significant increase of the rotational correlation time of the spin probe, indicating reduced motion in both G and F-actin. The orientation dependence of the electron paramagnetic resonance spectra in oriented F-actin filaments revealed an altered molecular order of the probe when the nucleotide was a Br-substituted one. The bound nucleotide affects the myosin S1 ATPase activation by actin; both  $V_{\max}$  and  $K_{\text{actin}}$  decreased significantly when the bound nucleotide of actin was Br<sup>8</sup>ADP.

Actin, regardless of its muscle or cytoplasmic origin, contains a non-covalently bound adenine nucleotide. G-actin binds ATP, which is known to be indispensable to the stability of the protein. Upon polymerization ATP is dephosphorylated to ADP. While the G-actin-bound ATP is readily exchangeable with external nucleotides, the ADP of F-actin is essentially non-exchangeable.

Considerable progress has recently been made in the localization of the nucleotide-binding site of actin. According to X-ray crystallographic data, ATP binds in the cleft between the smaller N-terminal and larger C-terminal lobes of actin [1]. Photoaffinity labeling experiments [2, 3] and proton NMR studies [4–6] show that the nucleotide interacts with several amino acid side-chains including Lys-336, Trp-356 and Tyr-306 in the C-terminal region, as well as with residues 115–118, 121–124 and 57–62 in the N-terminal part of actin. There is evidence of overlap between the nucleotide-binding site and the phalloidin-binding site, and of N and C-terminal lobes of actin being involved in the phalloidin binding, which stabilizes the structure of F-actin [5, 7].

In this report the internal motion of G and F-actin with Br<sup>8</sup>-substituted nucleotide (in which the rotation of the glycosidic bond is hindered) has been studied by measuring the rotational mobility of a paramagnetic probe attached to the C-terminal domain. From the experiments it can be concluded that the substituted bound nucleotide induced an increase in the rigidity of the internal structure of actin that is accompanied with a reduced activation on myosin S1 ATPase. The orientation of the probe on actin filaments and the effect of myosin fragments on the reorientation of the probe were also influenced by the modified bound nucleotide.

*Correspondence to* G. Hegyi, Biokémiai Tanszék, Eötvös Loránd Tudományegyetem, H-1088 Budapest, Puskin u. 3, Hungary

*Abbreviations.* S1, myosin subfragment-1; HMM, heavy meromyosin; Br<sup>8</sup>ADP, 8-bromoadenosine diphosphate.

*Enzyme.* Myosin ATPase, adenosine 5'-triphosphatase (EC 3.6.1.32).

## MATERIALS AND METHODS

Synthesis of Br<sup>8</sup>ATP was carried out as in [8] and the crude product was purified on a DEAE-Sephadex A-25 column and found to be homogeneous on HPLC.

*Preparation of Br<sup>8</sup>ATP–G-actin.* Actin was prepared according to [9]. After two polymerization cycles the F-actin pellet was homogenized in a solution containing 30 mM KCl, 2 mM Tris/HCl, pH 7.6 and ultracentrifuged again to remove the excess nucleotide. The washed F-actin pellet was homogenized for 15 min at 0°C in a solution containing 2 mM Tris/HCl, pH 7.6, 0.5 mM Br<sup>8</sup>ATP. After polymerization by 100 mM KCl and centrifugation, depolymerization in Br<sup>8</sup>ATP was repeated. The free nucleotide was removed by brief Dowex-1 treatment of 0°C [24]. In this way Br<sup>8</sup>ATP was incorporated into G-actin, and upon polymerization it was dephosphorylated to Br<sup>8</sup>ADP. The bound nucleotides were identified after deproteinization in 5% perchloric acid on a C<sub>18</sub> reverse-phase HPLC column with an eluent containing 0.05 M KH<sub>2</sub>PO<sub>4</sub> pH 6, 0.5 mM EDTA and 20% methanol.

Actin was spin-labelled in the F form with *N*-(1-oxyl-2,2,6,6-tetramethyl-4-piperidiny)maleimide, with one mole of spin label to one mole of actin, under continuous stirring for 120 min at 2°C. The reaction was terminated by pelleting the actin by ultracentrifugation. The pellet was depolymerized by homogenization and dialysis overnight. The degree of labeling varied between 0.2 mol and 0.5 mol label/mol actin. The label content was determined by comparing the intensities of the EPR signals of the denatured sample with the intensities of the signals from maleimide-label solutions of known concentration.

S1 was prepared as in [10] and heavy meromyosin (HMM) was prepared according to [11]. Protein concentrations were estimated from ultraviolet absorption using coefficients of 0.63 mg ml<sup>-1</sup> cm<sup>-1</sup> at 290 nm for actin [13], 0.6 mg ml<sup>-1</sup> cm<sup>-1</sup> at 280 nm for HMM and 0.8 mg ml<sup>-1</sup> cm<sup>-1</sup> at 280 nm for S1 [14].

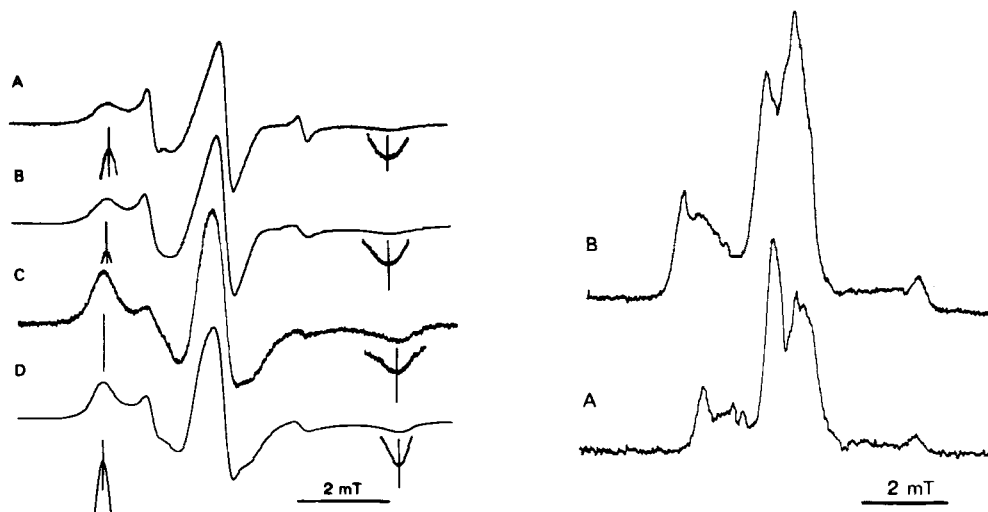


Fig. 1. Conventional (left) and saturation-transfer (right) EPR spectra of spin-labelled actin. Left: A, ATP–G-actin; B, Br<sup>8</sup>ATP–G-actin; C, ADP–F-actin; D, Br<sup>8</sup>ADP–F-actin. Actin concentration was 4.3 mg/ml, G-actin was measured in 0.5 mM ATP or Br<sup>8</sup>ATP, 2 mM Tris/HCl pH 8, and the samples were polymerized with 100 mM KCl for 1 h at room temperature. The insets with bars show the first and the last extrema at higher amplification. Right: A, ADP–F-actin; B, Br<sup>8</sup>ADP–F-actin. In spectrum A a component arising from a small amount of weakly immobilized label is also present

Actin-activated S1 ATPase activities were determined by measuring the released P<sub>i</sub> [12]. Assays were carried out in 0.75-ml volumes containing 60 μg S1, 80–500 μg actin, 20 mM Tris/acetate pH 7, 20 mM KCl, 2 mM MgCl<sub>2</sub> and 2 mM ATP, incubated at 25°C for 20 min.

EPR experiments were performed at room temperature with an ERS 220 X-band spectrometer (Center of Scientific Instruments, GDR). For conventional (V<sub>1</sub>) EPR technique 100-kHz field modulation (0.1–0.25 mT) and 10–20-mW microwave power were used in the ZSX cylindrical cavity with a flat cell of 500 μl capacity. Second harmonic absorption out-of-phase (V<sub>2</sub>) spectra were recorded with 50-kHz modulation (0.5-mT amplitude) and detection at 100 kHz. The out-of-phase setting was obtained by shifting the phase of the modulation field with a precision phase-shifter at low microwave power (1 mW) to obtain the minimum signal [15]. The saturation-transfer spectra were recorded at 85 mW microwave power, corresponding to an average microwave amplitude  $\langle H_1 \rangle$  of 0.025 mT in the central region of the flat cell (Zeiss, GDR) in the RSX rectangular cavity. The microwave magnetic field was determined with peroxyamine disulfonate ion radicals in the same sample cell as was used for the actin samples, according to [16]. The magnetic field calibration was performed with a nuclear magnetic resonance magnetometer (MJ-110R Radiopan, Poland).

*N*-(1-Oxyl-2,2,6,6-tetramethylpiperidiny)maleimide was a gift from Dr. K. Hideg (Central Laboratory, Pécs). All other reagents were analytical grade obtained from Reanal (Budapest).

## RESULTS

### Rotational motion of actin with bound Br<sup>8</sup>ATP

The conventional and saturation-transfer EPR spectral parameters are summarized in Table 1. The conventional EPR spectrum of G-actin could be interpreted as superposition of spectra arising from strongly and weakly immobilized labels. The weakly immobilized label did not account for more than 6–7% of the total EPR absorption (Fig. 1).

Table 1. EPR spectral parameters of the labelled actins

Rotational correlation times  $\tau_2$  were calculated for G-actins for the values of the  $2A'_{zz}$  using the Goldman equation [26], and for F-actins the saturation-transfer EPR spectra were evaluated according to Thomas et al. [15].  $2A'_{zz}$  is the hyperfine splitting constant,  $L''/L$  is the low-field spectral parameter and  $R_{\parallel}/R_{\perp}$  is the empirical order parameter

Labelled actin	$2A'_{zz}$	$\tau_2$		
	mT		μs	
ATP–G-actin	$6.328 \pm 0.05$	–	$0.016 (n = 8)$	
Br <sup>8</sup> ATP–g-actin	$6.434 \pm 0.05$	–	$0.025 (n = 5)$	
		$L''/L$		
ADP–F-actin	$6.755 \pm 0.03$	$0.65 \pm 0.07$	40	$(n = 8)$
Br <sup>8</sup> ADP–F-actin	$6.774 \pm 0.03$	$0.78 \pm 0.09$	80	$(n = 5)$
		$R_{\parallel}/R_{\perp}$		
ADP–F-actin pellet	$6.837 \pm 0.03$	$2.42 \pm 0.08$	100	$(n = 4)$
Br <sup>8</sup> ADP–F-actin pellet	$6.858 \pm 0.02$	$1.89 \pm 0.016$	100	$(n = 5)$

In order to obtain the rotational correlation time ( $\tau_2$ ) of the actin-bound label, according to McCalley et al. [25] we used sucrose to vary the solvent viscosity ( $\zeta$ ). The hyperfine splitting constant ( $2A'_{zz}$ ) at infinite viscosity was  $2A'_{zz} = 6.895 \pm 0.1$  mT, and 16 ns was calculated for the strongly immobilized maleimide spin label following Goldman and coworkers [26]. The plot of  $\tau_2^{-1}$  against  $T/\zeta$  ( $T$ , the absolute temperature) indicated that the strongly immobilized label did not have any significant rotational motion relative to the protein moiety, therefore  $\tau_2$  of the label can be considered as the rotational correlation time of the larger domain. In the samples of Br<sup>8</sup>ATP–G-actin a slightly but significant larger hyperfine splitting constant was measured indicating a slower rotational motion of the probe molecules (see Table 1).

Addition of KCl to a final concentration of 100 mM induced an increased immobilization of the strongly immobilized sites; for Br<sup>8</sup>ADP–F-actin the change in the separation of the outermost peaks was 0.34 mT after 1 h polymerization. The difference obtained in the mobility of ATP–

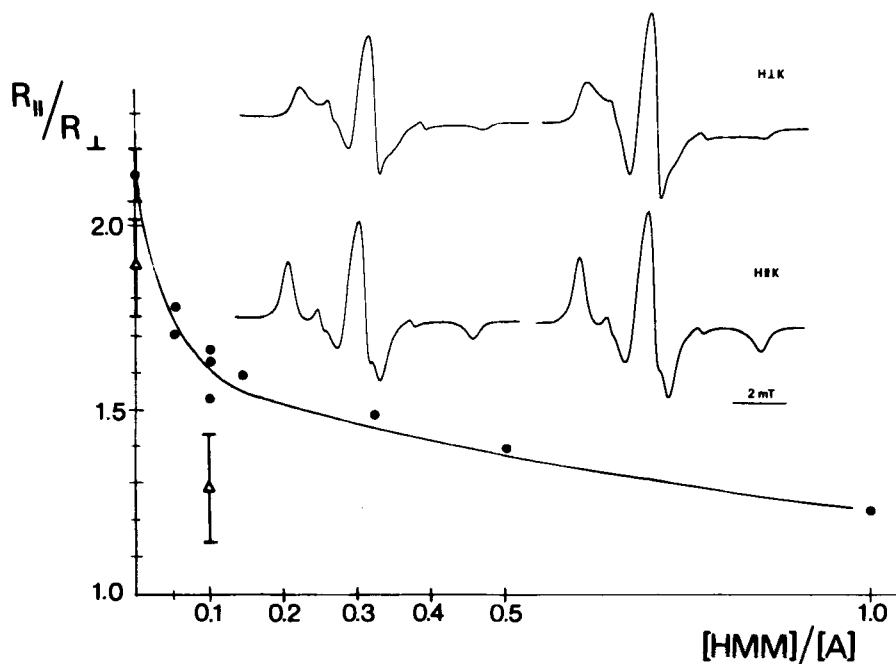


Fig. 2. Effect of HMM on the ordering of the probe in oriented F-actin filaments. (●) ADP-F-actin, (△) Br<sup>8</sup>ADP-F-actin. The inset shows the EPR spectra of oriented filaments. Upper spectra: filament axis was oriented perpendicular to the magnetic field. Bottom spectra: filament axis was oriented parallel to the magnetic field. Left: Br<sup>8</sup>ADP-F-actin; right: ADP-F-actin

G-actin and Br<sup>8</sup>ATP-G-actin increased after polymerization. From the saturation-transfer EPR spectra  $\tau_2$  values of 40  $\mu$ s and 80  $\mu$ s were obtained for the ADP-F-actin and Br<sup>8</sup>ADP-F-actin respectively, showing a considerable slowing down of the motion of the probe in Br<sup>8</sup>ADP-F-actin (Table 1).

#### Orientation dependence of the probe in the Br<sup>8</sup>ADP-F-actin

It is known from earlier experiments that the spin labels in oriented actin bundles exhibit a preferred orientation [20] and degree of the order parameter, defined as the ratio of the first peak heights in parallel and perpendicular orientation of the long axis of the actin filaments relative to the magnetic field. The peak heights are normalized to the second or to the fourth peaks (e.g.  $R_{\parallel} = I_{\parallel}^1/I_{\perp}^1$  or  $I_{\parallel}^4/I_{\perp}^4$ ) in the given experiments. Using the calibration curve of [23] we could conclude that the empirical order parameter ( $R_{\parallel}/R_{\perp}$ ) was significantly lower in Br<sup>8</sup>ADP-F-actin than in ADP-F-actin (Table 1 and Fig. 2). Moreover, in the case of Br<sup>8</sup>ADP-F-actin the maximal change of order parameter induced by HMM has been observed at lower HMM concentration than with the control actin (Fig. 2).

#### Effect of nucleotide bound to actin on the activation of myosin S1 ATPase

As double-reciprocal plots (Fig. 3) show the bound nucleotide affects both the  $K_{\text{actin}}$  and  $V_{\text{max}}$  of acto-S1 ATPase. Substitution of ADP for Br<sup>8</sup>ADP decreases  $K_{\text{actin}}$ :  $K_{\text{Br}^8\text{ADP-F-actin}}$  is 15.8  $\mu$ M, while  $K_{\text{ADP-F-actin}}$  is 34.8  $\mu$ M. Beyond the slightly increased affinity of actin to S1 there was also a significant decrease of  $V_{\text{max}}$  of the acto-S1 ATPase when the nucleotide bound to actin was Br<sup>8</sup>ADP.

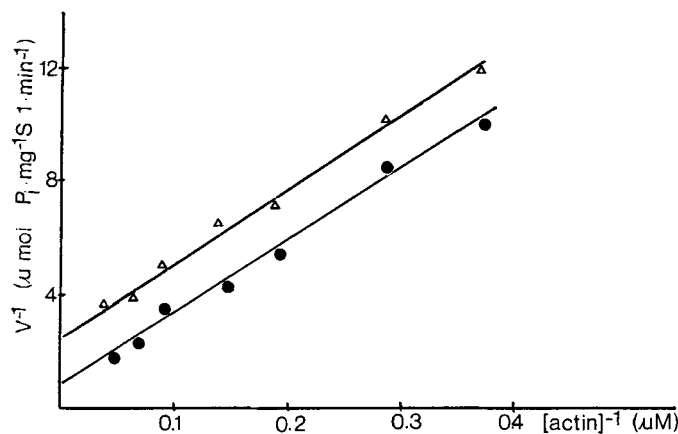


Fig. 3. Activation of S1 ATPase by ADP-F-actin and Br<sup>8</sup>ADP-F-actin. (●) ADP-F-actin, (△) Br<sup>8</sup>ADP-F-actin

#### DISCUSSION

Br<sup>8</sup>ATP and other ATP analogues, substituted at the C-8 atom of the purine ring by a bulky group, have hindered rotation around the glycosidic bond [17–19]. However these compounds seem to fit into the nucleotide-binding site of actin (under our experimental conditions a stoichiometric amount of Br<sup>8</sup>ATP was detected in G-actin) and when bound they behave similarly to unsubstituted ATP; G-actin with Br<sup>8</sup>ATP as bound nucleotide retains its polymerizability and the bound nucleotide analogue is dephosphorylated during polymerization, which is also the case for N<sup>3</sup>ATP [2]. However, our present study shows that the motional properties of actin changed when the conformationally restricted Br<sup>8</sup>ATP was the bound nucleotide. The reduced internal motion of the maleimide spin label that is attached to the Cys-374 [20] must be the consequence of the decreased internal motion of the

actin monomer itself, presumably as a result of the interdomain interaction of the bound nucleotide. It is assumed that the Cys-374 is not involved directly in the nucleotide-binding site since the distance between Cys-374 and the nucleotide-binding site is about 3 nm by fluorescence energy-transfer measurements [21, 22]. The remarkable increase of rotational correlation time of the probe in F-actin with Br<sup>8</sup>ADP can be interpreted as a result of the reduced flexibility of the monomers. Furthermore the orientation dependence of the EPR spectra of oriented F-actin filaments indicated a different molecular order of the probe. This difference can be explained by a change of the angle of the molecular *z* axis for the paramagnetic probe relative to the longer axis of the filaments. Thus a change of the torsional and flexing motions in Br<sup>8</sup>ADP–F-actin may also be the consequence of a slightly altered structure of these filaments.

This slightly altered structure of Br<sup>8</sup>ADP–F-actin influences the interactions of actin with HMM and S1. In the case of Br<sup>8</sup>ADP–F-actin the characteristic drop of the empirical order parameter, observed in the rigor complex of actin and HMM [23], was more pronounced than with the ADP–F-actin and, in the experiments for the activation of S1 ATPase by Br<sup>8</sup>ADP–F-actin, lower  $V_{\max}$  and  $K_{\text{actin}}$  values were found. The change of the kinetic parameters of the acto-S1 ATPase can be interpreted only by the above-mentioned altered dynamics of the actin since the 1–10  $\mu\text{M}$  concentration of free Br<sup>8</sup>ATP and Br<sup>8</sup>ADP added together with actin has not any effect on the acto-S1 ATPase under the given experimental conditions. (Note that the substrate of S1 ATPase was unsubstituted ATP in millimolar concentration.)

The change in the probe orientation and/or the slight torsion of Br<sup>8</sup>ADP–F-actin is supported by the measurement of the hyperfine splitting constant in the presence of increasing amounts of S1 (results are not shown). At a higher molar ratio (over 0.2) of S1 to ADP–F-actin, the  $2A'_{zz}$  spectral parameter showed an approximately linear decrease with the addition of S1. This is due to the shielding effect of the myosin fragments in the neighbourhood of the label (decreasing polarity, see [27]). In contrast, the interaction of S1 with Br<sup>8</sup>ADP–F-actin resulted only a slight increase of  $2A'_{zz}$  (immobilizing effect of S1) but the shielding effect of S1 at higher concentration was not observed. This also indicates that an induced distortion by the modified nucleotide may reorient the nitroxide group of the attached label.

From these results we conclude that the binding of Br<sup>8</sup>-nucleotides slows down the rotational motion of the probe by reducing the internal motion of actin moiety containing the probe. This effect can be mediated by direct interactions of the modified nucleotide with the C-terminal lobe of actin. However, on the basis of the several known interactions of bound nucleotide with the C and N-terminal parts of the molecule, we think it possible that the conformationally restricted nucleotide analogue, stiffly connecting the two lobes of actin, can also cause altered motional dynamics. The different segmental flexibility of actin filaments and/or the reduced internal motion of the monomers affect the interaction of actin with myosin fragments also.

These results also suggest that the F actin or the thin filaments having unsubstituted bound nucleotide are not rigid rods, and that the dynamics of actin are controlled at least

partially by the bound nucleotide. The degree of flexibility of the interlobe connection may be critical for the function of actin molecule. Weakening of this interaction (upon removal of nucleotide from G-actin) leads to the denaturation of the protein, but if gets too tight it may hinder the perfect actin–myosin interaction during the contraction cycle.

This work was supported by the National Scientific Research Foundation of Hungary (OTKA) grants 572 and 823. The authors thank Dr John Gergely for his helpful comments on the manuscript and Dr Kálmán Hideg for providing the maleimide spin label.

## REFERENCES

1. Kabsch, W., Mannherz, H. G. & Suck, D. (1985) *EMBO J.* **4**, 2113–2118.
2. Hegyi, G., Szilágyi, L. & Elzinga, M. (1986) *Biochemistry* **25**, 5793–5798.
3. Kuwayama, H. & Yount, R. G. (1986) *Biophys. J.* **49**, 454a.
4. Barden, J. A. & Kemp, B. E. (1987) *Biochemistry* **26**, 1471–1478.
5. Barden, J. A., Miki, M., Hambly, D. & dos Remedios, C. G. (1987) *Eur. J. Biochem.* **162**, 583–588.
6. Levine, B. A. & Moir, A. J. (1987) *J. Muscle Res. Cell Motil.* **8**, 72.
7. Vandekerckhove, J., Deboben, A., Nassal, M. & Wieland, T. (1985) *EMBO J.* **4**, 2815–2818.
8. Ikehara, M. & Uesugi, S. (1969) *Chem. Pharm. Bull. (Tokyo)* **17**, 348–354.
9. Spudich, J. A. & Watt, S. (1971) *J. Biol. Chem.* **246**, 4866–4872.
10. Weeds, A. G. & Taylor, R. S. (1975) *Nature (Lond.)* **257**, 54–56.
11. Lowey, S., Slayter, H. S., Weeds, A. G. & Baker, H. (1969) *J. Mol. Biol.* **42**, 1–29.
12. White, H. J. D. (1982) *Methods Enzymol.* **85B**, 700–701.
13. Houk, T. W. Jr & Ue, K. (1974) *Anal. Biochem.* **62**, 66–74.
14. Margossian, S. S. & Lowey, S. (1978) *Biochemistry* **17**, 5431–5439.
15. Thomas, D. D., Dalton, L. R. & Hyde, J. G. (1976) *J. Chem. Phys.* **65**, 3006–3024.
16. Fajer, P. & Marsh, D. (1982) *J. Magnet. Res.* **49**, 212–224.
17. Ikehara, M., Uesugi, S. & Yoshida, K. (1972) *Biochemistry* **11**, 830–836.
18. Sarma, M., Lee, C. H., Evans, F. E., Yathindra, N. & Sundaralingam, M. (1974) *J. Am. Chem. Soc.* **96**, 7337–7348.
19. Uesugi, S. & Ikehara, M. (1977) *J. Am. Chem. Soc.* **99**, 3250–3253.
20. Burley, R. H., Seidel, J. C. & Gergely, J. (1971) *Arch. Biochem. Biophys.* **146**, 597–602.
21. Miki, M. & Wahl, P. (1984) *Biochim. Biophys. Acta* **786**, 188–196.
22. Barden, J. A. & dos Remedios, C. G. (1987) *Eur. J. Biochem.* **168**, 103–109.
23. Belágyi, J., Gróf, P. & Pallai, G. (1979) *Acta Biochim. Biophys. Acad. Sci. Hung.* **14**, 293–296.
24. Strzelecka-Golaszewska, H. & Drabikowski, W. (1968) *Biochim. Biophys. Acta* **162**, 581–595.
25. McCalley, R. C., Shimishick, E. J. & McConnell, M. M. (1972) *Chem. Phys. Lett.* **13**, 115–119.
26. Goldman, S. A., Bruno, G. V. & Fred, J. H. (1972) *J. Phys. Chem.* **78**, 1858–1860.
27. Thomas, D. D., Seidel, J. C. & Gergely, J. (1979) *J. Mol. Biol.* **132**, 227–273.